HHS Public Access

Author manuscript

Pharm Res. Author manuscript; available in PMC 2019 January 02.

Published in final edited form as:

Pharm Res. ; 35(1): 6. doi:10.1007/s11095-017-2282-4.

Leukemia Inhibitory Factor-Loaded Nanoparticles with Enhanced Cytokine Metabolic Stability and Anti-Inflammatory Activity

Stephanie M. Davis[1], **Derek Reichel**[2], **Younsoo Bae**[2], and **Keith R. Pennypacker**[1]

[1]Department of Neurology, College of Medicine, University of Kentucky, 741 South Limestone, Lexington, Kentucky 40536, USA

[2]Department of Pharmaceutical Sciences, College of Pharmacy, University of Kentucky, 789 South Limestone, Lexington, Kentucky 40536, USA

Abstract

Purpose—To synthesize and assess the *in vitro* biological activity of nanoparticles containing leukemia inhibitory factor (LIF). These NanoLIF particles are designed to prolong the neuroprotective and anti-inflammatory actions of LIF in future preclinical studies of ischemic stroke.

Methods—LIF was packaged in nanoparticles made of poly(-ethylene glycol)-poly(lactic acid) (PEG-PLA) polymer to form LIF-loaded nanoparticles (NanoLIF). The surface of NanoLIF was also modified with the CD11b antibody (CD11b-NanoLIF) targeting activated peripheral macrophages to increase cytokine delivery to inflammatory macrophages. ELISA was used to quantify bioactive cytokine inside and releasing from NanoLIF. NanoLIF biological activity was measured using the M1 murine leukemia cell proliferation assay.

Results—NanoLIF and CD11b-NanoLIF had diameters of approximately 30 nm, neutral surface charge, and physicochemical stability retaining biological activity of the cytokine during incubation at 25°C for 12 h. NanoLIF particles released LIF relatively fast from 0 to 6 h after incubation at 37°C followed by slow release from 24 to 72 h according to a two-phase exponential decay model. NanoLIF and CD11b-NanoLIF significantly decreased M1 cell proliferation over 72 h compared to free LIF.

Conclusions—NanoLIF and CD11b-NanoLIF preserved the metabolic stability and biological activity of LIF *in vitro*. These results are promising to improve the therapeutic potential of LIF in treating neurodegenerative and inflammatory diseases.

Keywords

cytokine delivery; inflammation; macrophages; neurodegeneration; stroke

Corresponding author: Keith R. Pennypacker, keith.pennypacker@uky.edu.

INTRODUCTION

Leukemia inhibitory factor (LIF) is an anti-inflammatory cytokine that increases neural cell survival and improves motor skill function after permanent ischemic stroke. LIF plays an important role in controlling post-stroke pathological events, which involve the initial brain damage from 0 to 24 h and macrophage-mediated secondary immune responses from 24 to 72 h. We previously confirmed that LIF decreased neural cell degeneration and improved motor skill performance three days after stroke in rats during focal cerebral ischemia (1,2). LIF administered intravenously readily crossed the blood-brain barrier (BBB) using a saturable transport system because the transport rate of LIF crossing the BBB and blood-spinal cord barrier increases during CNS injury (3–5). However, LIF-dependent neuroprotection and motor skills were not sustained at later time points after stroke presumably due to a short blood half-life of approximately 2 h in the body (6). LIF also lost its bioactivity during storage following freeze-thaw cycles. However, a short *in vivo* half-life and biostability limit the therapeutic potential of LIF in attenuating brain damage and facilitating long-term recovery after stroke.

Monocytes/macrophages are one of the key effector cells in the post-stroke inflammatory response (7,8). The inflammatory response initiated by these peripheral immune cells results in a second wave of neurodegeneration. LIF causes peripheral macrophages to release anti-inflammatory cytokines that attenuate post-stroke neuroinflammation. As a result, the treatment of macrophages with LIF decreases inflammatory signaling and curbs additional neurodegeneration (9,10).

To enhance neuroprotection we have developed in this study LIF-loaded nanoparticles (NanoLIF) that can prolong the stability and activity of the cytokine for future *in vivo* use. To attenuate peripheral inflammation, NanoLIF is also modified on the surface with the CD11b antibody (CD11b-NanoLIF) that can bind to the CD11b membrane protein overexpressed on macrophages (11,12). CD11b-NanoLIF is expected to target activated peripheral and splenic macrophages to inhibit the secondary inflammation in the injured brain. Figure 1 illustrates a potential stroke treatment strategy that NanoLIF will slowly release LIF treating the initial brain damage while CD11b-NanoLIF will target macrophages to inhibit the secondary immune response. These nanoparticles are designed to increase the local concentration of LIF near stroke sites to enhance the transport of the cytokine into the injured brain. Liposomes, emulsions and other nanoparticle formulations were previously developed for delivery of LIF and other proteins to the brain. Although these nanoparticles have demonstrated feasibility to improve the bioactivity of LIF *in vivo*, their properties are not yet optimized with LIF for treatment of brain ischemia because the release of LIF from the nanoparticles was too fast or storage stability was extremely low in freeze-thaw cycles. In addition, existing LIF formulations often fail to target specific cells for selective LIF delivery. In contrast, NanoLIF and CD11b-NanoLIF are designed to overcome these limitations and improve LIF stability and bioactivity by sustained release and macrophage-targeted delivery of the cytokine.

Nanoparticles are widely used as delivery vehicles improving blood retention time, *in vivo* stability, and targeted delivery of various therapeutic agents (small molecule drugs,

nucleotide drugs, and proteins). Their surface is generally designed to be hydrophilic to prevent protein adsorption in the body, while the core is engineered to entrap various molecules. Previous studies confirmed that nanoparticles are large enough to avoid transcellular and paracellular diffusion through healthy blood vessels, yet they are small enough to cross the disrupted blood vessels found in damaged tissues with inflammation (13–16). We have reported that nanoparticles made from biocompatible polymer assemblies forming 20 ~ 50 nm micelles are particularly useful to protect therapeutic agents from precipitation, serum adsorption, phagocytic and renal clearance (17–19). We expect that nanoparticles will also protect LIF in the core from denaturation and rapid clearance in the body while delivering the cytokine to ischemic sites in the brain more efficiently to maximize and extend the therapeutic benefits of LIF in stroke treatment. The nanoparticles will be particularly useful to improve blood retention half-life of LIF for prolonged efficacy for future *in vivo* applications.

Based on this background, the current study focuses on investigating if nanoparticles will protect LIF in the core from denaturation and enhance the bioactivity of LIF by CD11b-mediated targeting of macrophages in *in vitro* M1 cell culture systems. Pharmaceutical benefits of encapsulating cytokines in nanoparticles are also discussed to develop new therapeutics for stroke treatment.

MATERIALS AND METHODS

Chemicals and Cells

α-Hydroxyl-ω-acetyl-poly(ethylene glycol)-poly(lactic acid) (PEG-PLA, 5–5.3 kDa) was purchased from Polymer Source (Quebec, Canada). p-Maleimidophenyl isothiocyanate (PMPI) and tris(2-carboxyethyl)phosphine (TCEP) were purchased from Sigma Aldrich (St. Louis, MO). CD11b antibody was purchased from Abcam (Cambridge, United Kingdom). Ethanol, PBS, RPMI-1640 cell culture medium, DMSO, desalting columns with 7.5 kDa molecular weight cutoff (MWCO), and spin filters with 100 kDa MWCO were purchased from Fisher Scientific (Waltham, MA). DuoSet ELISA kit for human LIF was purchased from R&D Systems (Minneapolis, MN). TIB-192 murine myeloid leukemia (M1) cells were purchased from ATCC (Manassas, VA). Cells were cultured in a humidified condition at 37°C in 5% CO_2 following the ATCC recommendations. Heat-inactivated fetal bovine serum, 0.4% Trypan Blue solution, and penicillin/streptomycin solution were purchased from Corning (Manassas, VA). Recombinant human LIF was purchased from Prospec-Tany Technogene (New Brunswick, NJ).

Synthesis of Antibody-Conjugated PEG-PLA Polymer

CD11b antibody was conjugated to PEG-PLA following the two-step reaction shown in Fig. 2. First, PEG-PLA and PMPI were reacted in DMSO overnight at room temperature. PMPI-activated PEG-PLA was purified twice by desalting column and collected by freeze drying. Next, PMPI-activated and regular PEG-PLA were mixed in ethanol at 9:1 (*w*/w) and the solution was titrated into an equal volume of PBS. Ethanol was removed from the solution under nitrogen flow at room temperature to prepare surface-activated nanoparticles. CD11b antibody was then conjugated to the surface of nanoparticles by using TCEP in PBS for 2 h

at room temperature. The reaction aimed for a 1.0% molar substitution of CD11b antibody to PEG-PLA in polymer micelles. CD11b-conjugated nanoparticles were purified by centrifugal filtration and stored in solution. Antibody conjugation was verified by proton NMR spectroscopy (Varian 400 MHz).

Preparation of NanoLIF and CD11b-NanoLIF

NanoLIF and CD11b-NanoLIF were prepared by a solvent evaporation method. Briefly, PEG-PLA polymer or CD11b-conjugated PEG-PLA polymer was dissolved in ethanol (2 mg/ml) and mixed with LIF in water (5 μg/ml) to prepare 1 ml of 1:1 ethanol: water mixed solvent. Ethanol was evaporated under nitrogen flow for 2 h, and the solution was lyophilized to prepare NanoLIF. Freeze-dried NanoLIF and CD11b-NanoLIF were reconstituted in PBS to quantify the concentration of active LIF remaining in the solution by ELISA. The loading efficiency (LE) of LIF was determined from the weight ratio of LIF to nanoparticles, and the encapsulation efficiency (EE) of LIF was determined from the weight ratio of entrapped LIF to added LIF. Empty particles were prepared as a negative control by repeating the solvent evaporation method without adding LIF. PGLA nanoemulsions containing LIF were prepared as a positive control as previously described (20).

Characterization of Physicochemical Properties

The diameter and surface charge of NanoLIF were determined by Zetasizer Nano (Malvern, UK). The critical micelle concentration (CMC) of NanoLIF in solution was determined by using a pyrene method. Stock solutions of polymer (2 mg/ml, PBS) and pyrene (30 μM, acetone) were prepared. Pyrene solution (2 μL) was added to serial dilutions of polymer solutions (100 μL) and incubated overnight at 37°C. The ratio of pyrene fluorescence peaks I1 (Ex 334 nm/Em 372 nm) and I3 (Ex 334 nm/Em 383 nm) was plotted against polymer concentrations, and the CMC was determined from the inflection point of the graph.

ELISA Quantification and Verification of Bioactive LIF

We first confirmed that the Human LIF ELISA kit was specific for active LIF and insensitive to denatured LIF. One hundred pg of LIF that was stored at 4°C was quantified according to the kit instructions. The same quantity of LIF that had been incubated at 100°C for 10 min served as a negative control. The percentage of biologically active LIF was calculated by dividing the quantity of LIF detected by ELISA by the total LIF

Quantification of LIF in NanoLIF Particles

Human LIF ELISA kit was used to quantify bioactive LIF in PGA-PLA nanoparticles that were conjugated to CD11b or left unlabeled. We compared the concentrations of LIF in the NanoLIF particles to nanoemulsions made of poly(D,L-lactide-co-glycolide) (PLGA) and poly(vinyl alcohol) (PVA), which had been reported in previous studies as an injection formulation of LIF (21). The DuoSet. Empty NanoLIF and free LIF were used as negative controls for the nanoparticles and cytokine in the ELISA.

Determination of LIF Release from Nanoparticles

Nanoparticles entrapping LIF were reconstituted in PBS at 1 mg/ml and mixed with M1 cell complete medium (RPMI-1640 medium containing 10% heat-inactivated FBS and 1% penicillin/streptomycin solution). Samples were taken at 2, 4, 6, 24,48, and 72 h after incubation to calculate the LIF release kinetics. LIF concentrations were quantified by ELISA. The percentage of total LIF released was calculated at each time point. Free LIF was used as a positive control for the NanoLIF. The concentrations of LIF remaining in the supernatant at various time points during the incubation were used to calculate the percentage of LIF remaining in the nanoparticles. Nonlinear regression analysis using an F-test was performed to determine the release of LIF by a one phase exponential decay or two phase exponential decay pattern.

LIF Bioactivity Assessment

The bioactivity of LIF in the nanoparticles was determined as previously described with several modifications (22). TIB-192 murine leukemia (M1) cells were plated in 24 well culture plates at an initial density of 500,000 cells/well in 1 ml of M1 complete cell medium. Cells were treated with PBS, LIF (20 ng), NanoLIF (7.7 ng), and CD11b-NanoLIF (4.1 ng). Equal volumes of empty NanoLIF and CD11b-NanoLIF were used to treat M1 cells to ensure that the empty particles had no negative effect on cellular proliferation. Cells were incubated at 37°C with 5% CO_2 for 72 h, and diluted in an equal volume of 0.4% trypan blue dye solution in PBS. The number of viable cells was counted with a hemocytometer. These values were used to calculate the cellular proliferation rate as a percentage of the PBS treatment group. Results were compiled from three experiments utilizing M1 cells from different passages.

LIF Stability Assessment

Free NanoLIF and CD11b-NanoLIF were dissolved in sterile PBS and incubated at 25°C for 12 h. Free cytokine and NanoLIF samples stored at 4°C for 12 h were used to control for the variation in temperature. The proliferation rates of the LIF and NanoLIF-treated groups were expressed as a percentage of the PBS-treated group for each experiment. The experiments were repeated in triplicate using cells with different passage numbers. Nanoparticle solutions went through one freeze-thaw cycle were also used for comparison. NanoLIF and nanoemulsions were lyophilized and incubated at 37°C for 24 h. These ‘pre-treated’ NanoLIF (20 ng) was used to treat M1 cells to determine changes in LIF bioactivity following 72 h incubation.

Statistical Analysis

All statistical tests were performed by using GraphPad Prism (La Jolla, CA). Data in all figures and tables was expressed as the mean ± standard deviation. Experiments containing three or more treatment groups were analyzed using a one-way or two-way ANOVA followed by the protected Fisher’s LSD post hoc test. Data containing two treatment groups was analyzed by using an independent student’s t test. Welch’s correction was applied in the case of unequal variances between treatment groups. All reported p values are one-tailed. A p value of <0.05 was considered significant.

RESULTS

CD11b Antibody Conjugation to PEG-PLA

NMR confirmed CD11b (0.84 ppm, s; 1.05 ppm, s; 1.22 ppm, s; 1.27 ppm, s; 2.08 ppm, t; 2.70 ppm, s; 3.15 ppm, s; 4.18 ppm, s; 4.45 ppm, s; 4.51 ppm, s; 6.75 ppm, t; 7.15 ppm, t) conjugated to PEG-PLA (1.47 ppm, d; 3.54 ppm, s; 5.15 ppm, m). Peak ratios of CD11b to PEG-PLA indicated a 0.9% antibody substitution yield. The reaction had a 90% molar substitution yield, based on a comparison of measured molar antibody substitution to the theoretical substitution.

Nanoparticle Characterization

An average diameter of NanoLIF was 40 ~ 52 nm while CD11b-NanoLIF had a diameter 20% smaller than unlabeled NanoLIF (Table I). Both NanoLIF and CD11b-NanoLIF showed neutral surface charge. The CMC of LIF-loaded nanoparticles was <100 μg/ml, which is low enough to ensure particle stability *in vitro* and *in vivo* applications. Noticeably, the CMC of antibody-free NanoLIF was 3-fold greater than CD11b-NanoLIF. NanoLIF showed <2% (*w*/w) LIF loading and CD11b-NanoLIF had two times greater LIF entrapment in comparison to antibody-free NanoLIF (Table II).

Improved LIF Stability

ELISA was sensitive enough to detect 7.8 pg of free bioactive LIF in solution, and the assay confirmed that 77.5% of LIF in the original sample after one freeze-thaw cycle was biologically active. LIF incubated at 100°C for 10 minutes completely lost its bioactivity (Fig. 3). ELISA revealed that nanoparticles protected LIF more effectively than nanoemulsions following lyophilization and freeze-thaw cycles of initial optimization experiments. Pre-treated NanoLIF contained more bioactive LIF than the purified nanoemulsion sample in larger scale preparation experiments ($t = 5.182$, df = 2, $p = 0.0176$; Fig. 4). NanoLIF and CD11b-NanoLIF contained 222 ng and 331 ng of biologically active LIF per mg particles, but there was no statistical significance between the values ($t = 1.766$, df = 2; $p = 0.1097$; Fig. 5).

Sustained Release of LIF from Nanoparticles

Free LIF incubated in RPMI-1640 complete cell culture medium at 37°C with 5% CO_2 did not significantly altered the concentration of biologically active LIF from 0 to 72 h after the start of the incubation period ($F_{6,2,12} = 1.681$; $p = 0.2090$). However, NanoLIF changed the total released LIF concentration over this time period and demonstrated a gradual release of LIF (Fig. 6, $F_{13,2,26} = 9.347$; $p < 0.0001$). NanoLIF released cytokine at a sustained rate, and the release half-life was approximately 30 h, which was a significant improvement compared to the nanoemulsions (< 2 h). NanoLIF released approximately 14% of LIF at a fast rate in the initial stage (< 6 h) and slowed down the cytokine release in the late stage. NanoLIF completely released LIF in 72 h (Table III). These results were fitted to first-order and second-ordered exponential curves. The two-phase release profile better fitting the release kinetics of the NanoLIF ($F_{3,19} = 4.164$; $p = 0.020$; Fig. 7) suggested that NanoLIF released

the cytokine binding weakly to the nanoparticle shell or core-surface interface first and the LIF entrapped in the core of the particle later.

Enhanced LIF Bioactivity from Prolonged Incubation at 25°C.

Figure 3 shows that NanoLIF protects the free LIF during lyophilization and retains LIF bioactivity during incubation at 25°C for 12 h. Biological activity of free LIF decreased during incubation at 25°C, but the cytokine entrapped in nanoparticles showed significantly greater bioactivity than free LIF ($t = 7.375$, df = 4, $p = 0.0009$; Fig. 8a). In addition, the M1 cells treated with NanoLIF for 12 h at 25°C showed significantly lower rates of proliferation compared to cells treated with pre-incubated LIF ($t = 2.270$, df = 6, $p = 0319$; Fig. 8b). Although NanoLIF successfully protected LIF from incubation at 25°C, the results of the ELISA showed no significant difference in LIF bioactivity between NanoLIF formulations frozen/thawed once or freshly prepared from a frozen stock solution at −20°C ($t = 0.3940$, df = 4, $p = 0.3568$; Fig. 9a). M1 cell proliferation reduced after the freeze-thaw cycle, but this trend did not reach statistical significance ($t = 0.7343$, df = 8, $p = 0.2419$; Fig. 9b).

Effective Inhibition of M1 Cell Proliferation by NanoLIF and CD11b-NanoLIF

LIF and NanoLIF significantly altered the rate of M1 proliferation ($F_{5,12} = 8.592$, $p = 0.0012$). 20 ng of LIF significantly reduced the proliferation rate compared to the PBS group (*$p < 0.05$). NanoLIF (*p < 0.05) and CD11b-NanoLIF (**$p < 0.01$) significantly reduced the proliferation rate of the M1 cells. The rates of proliferation for cells treated with empty unlabeled NanoLIF (#p < 0.05) or empty CD11b-NanoLIF (^$p < 0.0001$) were significantly greater than rates of proliferation for cells treated with their LIF-containing counterparts. However, there was no significant difference in proliferation between cells treated with PBS and cells treated with empty NanoLIF and CD11b-NanoLIF (Fig. 10a). Due to the difference in cytokine entrapment efficiency between the between the NanoLIF and CD11b-NanoLIF micelles, the proliferation rates for each treatment group calculated the normalized % decrease in M1 cell proliferation per ng of LIF in each sample. There was a significant difference in the efficacies of LIF, NanoLIF, and CD11b-NanoLIF ($F_{2,6} = 20.69$, $p = 0.0020$). NanoLIF treatment yielded a significantly higher decrease in M1 proliferation per ng of LIF compared to LIF alone (**p < 0.01). However, the CD11b-NanoLIF yielded the highest decrease in M1 proliferation per ng LIF, which was significantly greater than the decrease in proliferation observed with LIF (*p < 0.05) and NanoLIF (#p < 0.05; Fig. 10b).

DISCUSSION

Stroke treatment requires therapeutics that concurrently reduce inflammation and promote neural cell survival. We previously reported that systemic administration of LIF to rats during focal cerebral ischemia diminishes degeneration of oligodendrocytes and neurons and improves functional recovery (1,2). Despite its therapeutic potential, LIF showed short blood retention time with a half-life of only 2 h due to its multiple disulfide domains and its tight regulation by serum proteases (6). We also found that LIF was prone to denaturation losing bioactivity during storage at 25°C, *in vitro* assays at 37°C, or even freeze-thaw cycles. Poor stability and bioactivity limit therapeutic benefits of LIF as a potential therapeutic for effective stroke treatment.

After encapsulation of LIF in nanoparticles in PEG-PLA nanoparticles the LIF-loaded nanoparticles not only increased potency but also protected the cytokine from thermal degradation. NanoLIF released LIF over an extended time with a release half-life of approximately 30 h well past its limited stability. Moreover, CD11b-conjugated NanoLIF retained these pharmaceutical advantages over free LIF. These results suggest that NanoLIF and CD11b-NanoLIF in combination will improve the efficacy of LIF as a therapeutic agent modulating the complicated pathological events involved with stroke. For instance, NanoLIF releasing LIF slowly near the injured brain sites can prolong therapeutic efficacy suppressing initial brain damage while CD11b-NanoLIF target macrophages and microglia triggering the secondary immune responses to the brain in the later stage.

Data suggests that NanoLIF will overcome limitations of other nanoparticle formulations previously developed, such as nanoemulsions containing LIF. Previously, nanoemulsions containing LIF were labelled with CD4 antibodies for delivery of LIF to T cells (20). We initially prepared LIF-loaded nanoemulsions, but we found that activity of LIF decreased significantly after loading compared to micelles prepared in a similar manner (1 ng/ml in nanoemulsions s 20 ng/ml in NanoLIF). Furthermore, previous studies have shown a low concentration of encapsulated LIF within the nanoemulsions (1 ng/ml) (20). On the other hand, NanoLIF entrapped up to 331 ng/ml LIF. Increased drug loading of NanoLIF will allow for the injection of larger amounts of cytokine to better test the therapeutic potential of LIF.

Addition of CD11b antibody decreased nanoparticle size and increased nanoparticle stability, possibly due to alteration of the PEG shell. CD11b antibodies could disrupt PEG chains in the nanoparticle corona because 48 kDa antibodies are bulkier than 5 kDa PEG. This theoretical mechanism explains why CD11b-NanoLIF nanoparticles had a smaller diameter and lower CMC than PEG-PLA nanoparticles (Table I). CD11b-NanoLIF with increased stability was able to entrap 50% more bioactive LIF than antibody-free NanoLIF. Antibody conjugation did not adversely affect the LIF-induced growth inhibition of M1 cells.

This study shows that LIF encapsulated in nanoparticles is more efficacious than free LIF in inhibiting M1 cell growth. CD11b-NanoLIF is designed to attach to activated macrophages and increase the probability of released LIF binding to its receptor on these cells.. Park *et al.* previously targeted naive T lymphocytes using CD4 antibody-conjugated nanoparticles containing LIF (20). These targeted nanoparticles were successful in treating a rodent model of multiple sclerosis, which is characterized by T cell-mediated damage of white matter (21).

CD11b-NanoLIF should be effective in the treatment of other macrophage-based diseases because LIF alters the phenotype of macrophages from inflammatory to anti-inflammatory. For example, macrophage activation syndrome is a serious condition caused by the over-activation of macrophages. Only broad spectrum anti-inflammatory agents, such as glucocorticoids and cyclosporine, have provided the remedy (23,24), but these drugs also increase the risk of opportunistic infections by causing widespread immunosuppression (25). CD11b-NanoLIF would be an ideal therapeutic in targeting these inflammatory

macrophages to diminish the detrimental consequences. Moreover, NanoLIF can be modified with other antibodies to enhance its effects in a cell specific manner.

We expect that protecting LIF with nanoparticles should dramatically improve motor skills in human patients. The prolonged release of LIF from the nanoparticle will further enhance this agent's therapeutic efficacy. CD11b-NanoLIF will decrease inflammation by targeting activated peripheral macrophages LIF released into the bloodstream will traverse the blood brain barrier via specific transporters and enter the injured brain. LIF release from NanoLIF in the brain will activate neuroprotective signaling in stroke-compromised oligodendrocytes and neurons (Figure 1). This approach is not restricted to stroke, but would be applicable to other brain injuries or organ pathologies that require inhibition of inflammation and/or cellular protection.

CONCLUSIONS

In this work, we developed LIF-loaded nanoparticles (NanoLIF) to improve the pharmaceutical and therapeutic properties of the cytokine for stroke treatment. NanoLIF effectively protects LIF against temperature changes (25° C and 37°C) and facilitated sustained release of the cytokine over 72 h. NanoLIF and CD11b-NanoLIF inhibit M1 cell proliferation at a significantly higher efficacy than free LIF alone. CD11b-NanoLIF that can target cells expressing CD11b antigen such as inflammatory macrophages may block the peripheral immune response and provide neuroprotection by releasing LIF to protect oligodendrocytes and neurons in the stroke-injured hemisphere for future clinical applications.

ACKNOWLEDGMENTS AND DISCLOSURES

The following funding sources were used to support this project: Project 5R01NS091146–03 from the National Institute of Neurological Disorders and Stroke, University of Kentucky College of Medicine.

ABBREVIATIONS

BBB	Blood-brain barrier
CD11b	Cluster of differentiation 11b
CMC	Critical micelle concentration
DLS	Dynamic light scattering
EE	Encapsulation efficiency
LE	Loading efficiency
LIF	Leukemia inhibitory factor
MWCO	Molecular weight cutoff
NanoLIF	LIF-loaded nanoparticles
PEG-PLA	Poly(ethylene glycol)-poly(lactic acid)

PLGA	Poly(D,L-lactide-co-glycolide)
PMPI	P-maleimidophenyl isothiocyanate
PVA	Poly (vinyl alcohol)
TCEP	Tris(2-carboxyethyl)phosphine

REFERENCES

1. Rowe DD, Collier LA, Seifert HA, Chapman CB, Leonardo CC, Willing AE, et al. Leukemia inhibitory factor promotes functional recovery and oligodendrocyte survival in rat models of focal ischemia. Eur J Neurosci. 2014;40:3111–9. [PubMed: 25041106]
2. Davis SM, Collier LA, Leonardo CC, Seifert HA, Ajmo CT, Pennypacker KR. Leukemia inhibitory factor protects neurons from ischemic damage via upregulation of superoxide dismutase 3. Mol Neurobiol. 2017;54(1):608–22. [PubMed: 26746670]
3. Pan W, Cain C, Yu Y, Kastin AJ. Receptor-mediated transport of LIF across blood–spinal cord barrier is upregulated after spinal cord injury. J Neuroimm. 2006;174(1–2):119–25.
4. Pan W, Yu C, Hsuchou H, Zhang Y, Kastin AJ. Neuroinflammation facilitates LIF entry into brain: role of TNF. Am J Physiol Cell Physiol. 2008;294(6):C1436–42. [PubMed: 18385284]
5. Pan W, Kastin AJ, Brennan JM. Saturable entry of leukemia inhibitory factor from blood to the central nervous system. J Neuroimmunol. 2000;106(1–2):172–80. [PubMed: 10814795]
6. Gunawardana DH, Basser RL, Davis ID, Cebon J, Mitchell P, Underhill C, et al. A phase I study of recombinant human leukemia inhibitory factor in patients with advanced cancer. Clin Cancer Res. 2003;9(6):2056–65. [PubMed: 12796368]
7. Kochanek PM, Hallenbeck JM. Polymorphonuclear leukocytes and monocytes/macrophages in the pathogenesis of cerebral ischemia and stroke. Stroke. 1992;23(9):1367–79. [PubMed: 1519296]
8. Ajmo CT, Jr, Vernon DO, Collier L, Hall AA, Garbuzova-Davis S, Willing A, et al. The spleen contributes to stroke-induced neurodegeneration. J Neurosci Res. 2008;86:2227–34. [PubMed: 18381759]
9. Duluc D, Delneste Y, Tan F, Moles MP, Grimaud L, Lenoir J, et al. Tumor-associated leukemia inhibitory factor and IL-6 skew monocyte differentiation into tumor-associated macrophage-like cells. Blood. 2007;110(13):4319–30. [PubMed: 17848619]
10. Jeannin P, Duluc D, Delneste Y. IL-6 and leukemia-inhibitory factor are involved in the generation of tumor-associated macrophage: regulation by IFN-gamma. Immunotherapy. 2011;3(4 Suppl):23–6.
11. Chen H, Chopp M, Zhang RL, Bodzin G, Chen Q, Rusche JR, et al. Anti-CD11b monoclonal antibody reduces ischemic cell damage after transient focal cerebral ischemia in rat. Ann Neurol. 1994;35(4):458–63. [PubMed: 8154873]
12. Zhang ZG, Chopp M, Tang WX, Jiang N, Zhang RL. Postischemic treatment (2–4 h) with anti-CD11b and anti-CD18 monoclonal antibodies are neuroprotective after transient (2 h) focal cerebral ischemia in the rat. Brain Res. 1995;698(1–2):79–85. [PubMed: 8581506]
13. Fang J, Nakamura H, Maeda H. The EPR effect: unique features of tumor blood vessels for drug delivery, factors involved, and limitations and augmentation of the effect. Adv Drug Deliv Rev. 2011;63(3):136–51. [PubMed: 20441782]
14. Maeda H, Matsumura Y. EPR effect based drug design and clinical outlook for enhanced cancer chemotherapy. In. Adv Drug Deliv Rev: Elsevier; 2011; p. 129–130.
15. Maruyama K Intracellular targeting delivery of liposomal drugs to solid tumors based on EPR effects. Adv Drug Deliv Rev. 2011;63(3):161–9. [PubMed: 20869415]
16. Torchilin V Tumor delivery of macromolecular drugs based on the EPR effect. Adv Drug Deliv Rev. 2011;63(3):131–5. [PubMed: 20304019]
17. Ponta A, Bae Y. Tumor-preferential sustained drug release enhances antitumor activity of block copolymer micelles. J Drug Target. 2014;22(7):619–28. [PubMed: 24766185]

18. Lee HJ, Ponta A, Bae Y. Polymer nanoassemblies for cancer treatment and imaging. Ther Delivery. 2010;1(6): 803–17.
19. Bae Y, Kataoka K. Intelligent polymeric micelles from functional poly (ethylene glycol)-poly (amino acid) block copolymers. Adv Drug Deliv Rev. 2009;61(10):768–84. [PubMed: 19422866]
20. Park J, Gao W, Whiston R, Strom TB, Metcalfe S, Fahmy TM. Modulation of CD4+ T lymphocyte lineage outcomes with targeted, nanoparticle-mediated cytokine delivery. Mol Pharm. 2011;8(1): 143. [PubMed: 20977190]
21. Rittchen S, Boyd A, Burns A, Park J, Fahmy TM, Metcalfe S, et al. Myelin repair *in vivo* is increased by targeting oligodendrocyte precursor cells with nanoparticles encapsulating leukaemia inhibitory factor (LIF). Biomaterials. 2015;56: 78–85. [PubMed: 25934281]
22. Metcalf D The leukemia inhibitory factor (LIF). The International Journal of Cell Cloning. 1991;9(2):95–108. [PubMed: 1645391]
23. Mouy R, Stephan J-L, Pillet P, Haddad E, Hubert P, Prieur A-M. Efficacy of cyclosporine A in the treatment of macrophage activation syndrome in juvenile arthritis: report of five cases. J Pediatr. 1996;129(5):750–4. [PubMed: 8917244]
24. Grom AA, Mellins ED. Macrophage activation syndrome: advances towards understanding pathogenesis. Curr Opin Rheumatol. 2010;22(5):561. [PubMed: 20517154]
25. Hofflin JM, Potasman I, Baldwin JC, Oyer PE, Stinson EB, Remington JS. Infectious complications in heart transplant recipients receiving cyclosporine and corticosteroids. Ann Intern Med. 1987;106(2):209–16. [PubMed: 3541723]

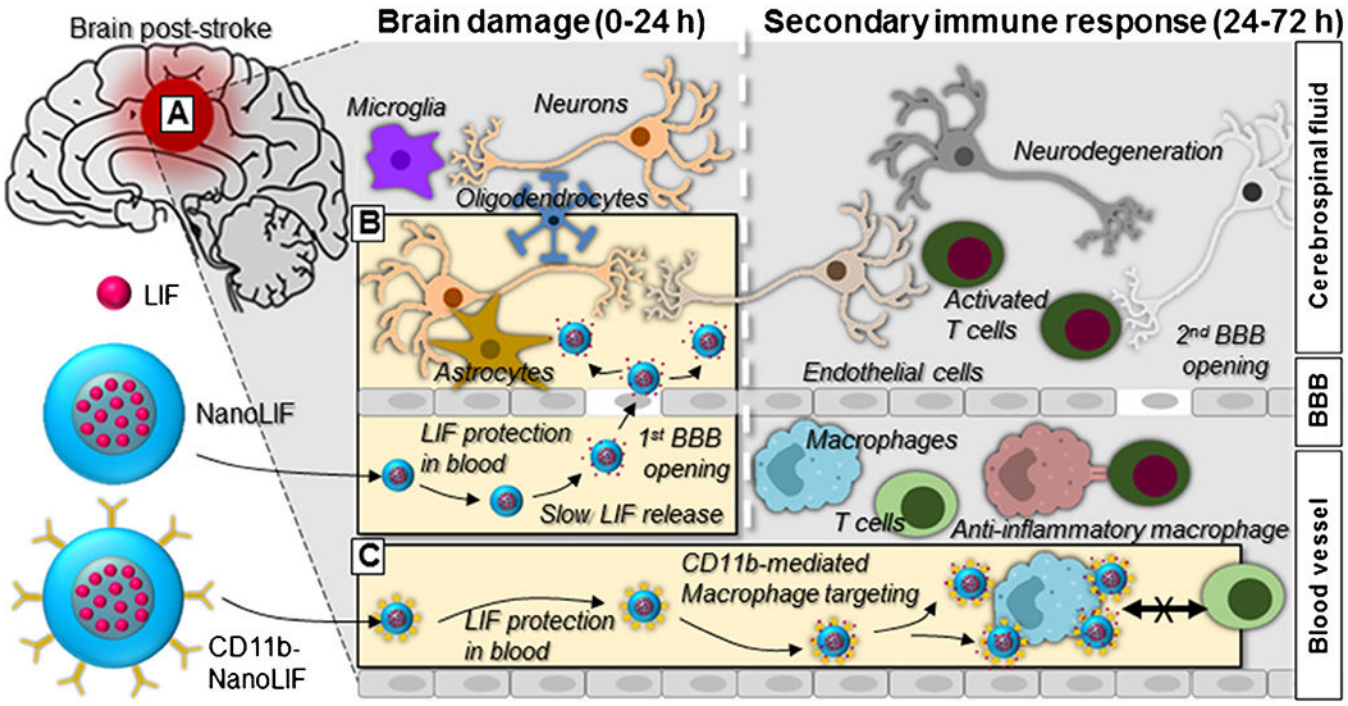

Fig. 1.

Post-stroke pathological events in the brain and novel therapeutic approach using NanoLIF (**a**) Neurodegeneration involves acute brain damage in the early stage after stroke followed by secondary immune response due to macrophage activation. (**b**) NanoLIF releasing LIF in the blood and damaged brain sites for a prolonged time is expected to increase concentrations and therapeutic efficacy of the cytokine. (**c**) CD11b-NanoLIF targeting inflammatory macrophages hold promise to suppress secondary immune response and thus improve stroke treatment and patient recovery

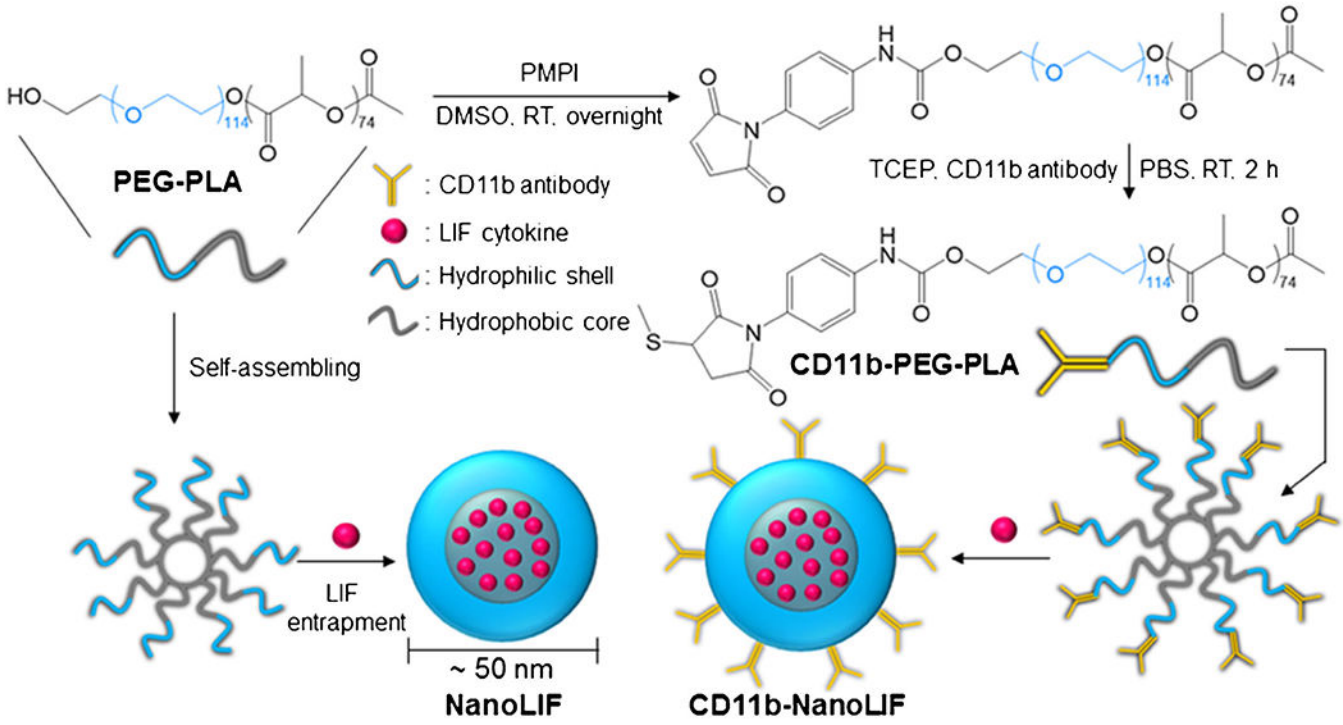

Fig. 2.
Synthesis of NanoLIF and CD11b-NanoLIF

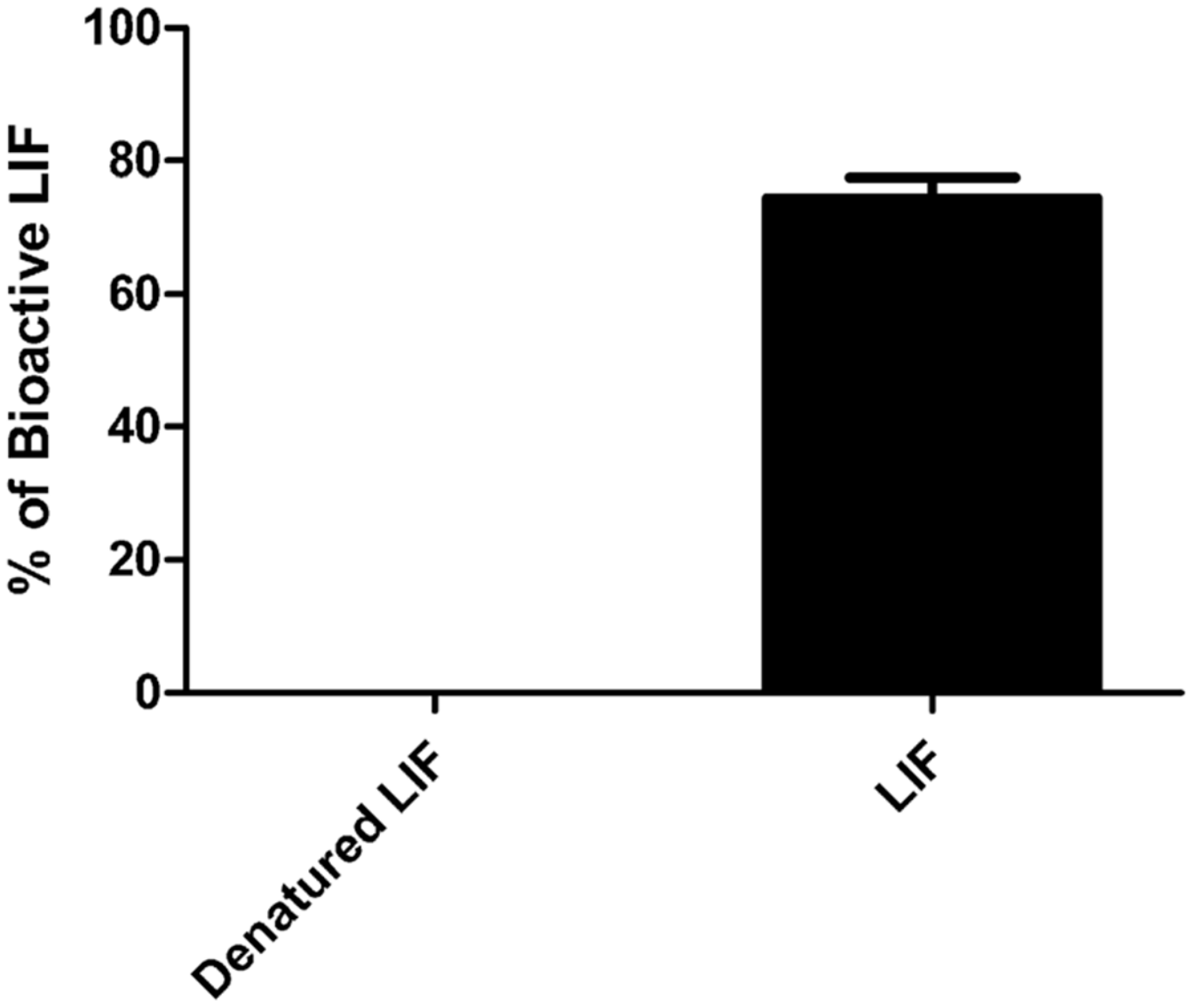

Fig. 3.

Seventy-seven percent of the LIF that was stored at 4°C was recognized as biologically active LIF but none of the denatured LIF was detected by the ELISA. All measurements are reported as mean ± standard error of the mean (n = 3 measurements per sample).

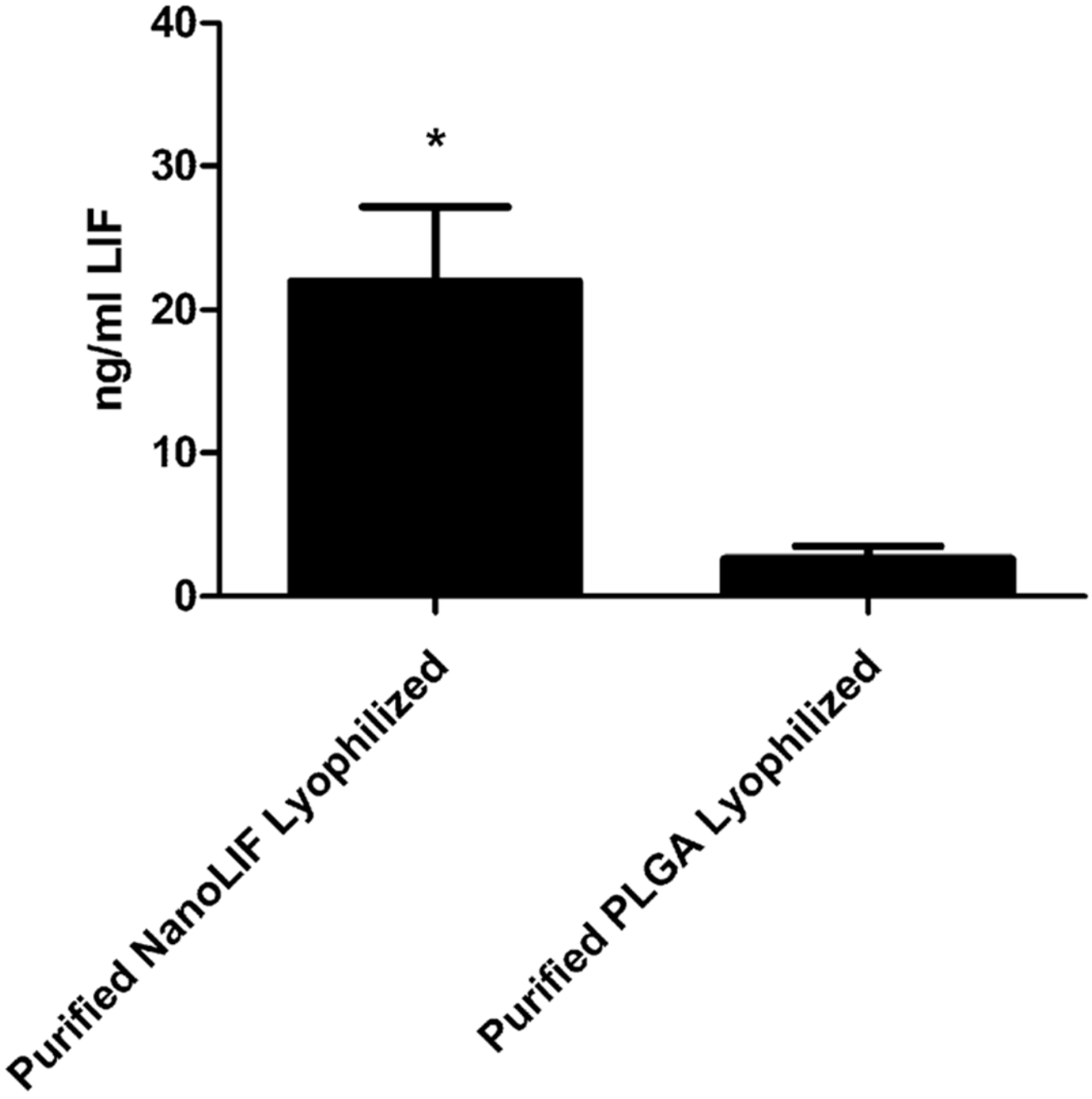

Fig. 4.

The purified NanoLIF samples that were lyophilized after processing had significantly higher concentration of encapsulated LIF compared to the purified PGLA nanoemulsions that were preserved via lyophilization (*$p < 0.05$; $n = 2$ measurements per sample).

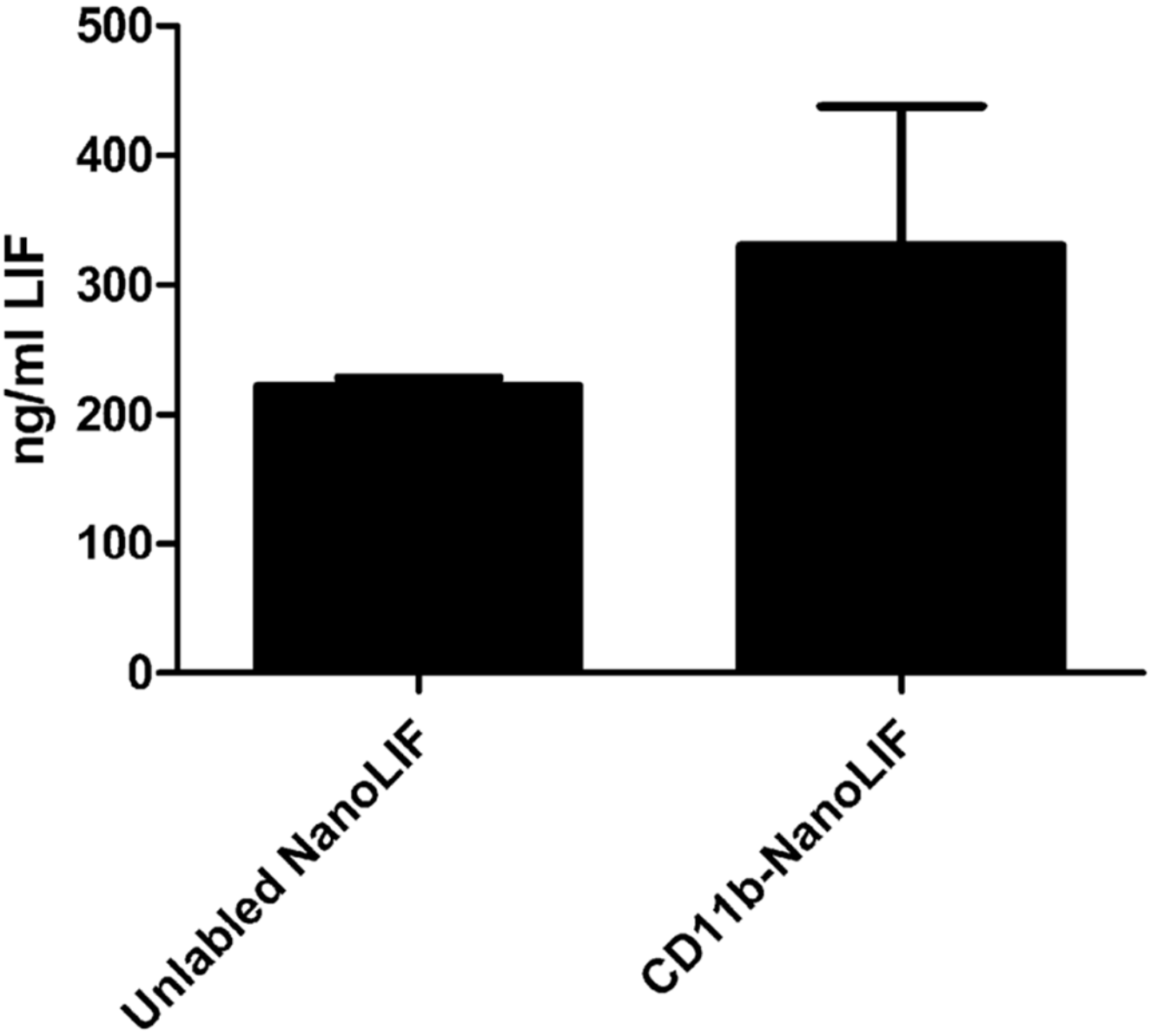

Fig. 5.

The unlabeled NanoLIF particles contained approximately 222 ng/ml of biologically active LIF and the CD11b-NanoLIF particles contained approximately 33 1 ng/ml (n = 3 measurements per sample).

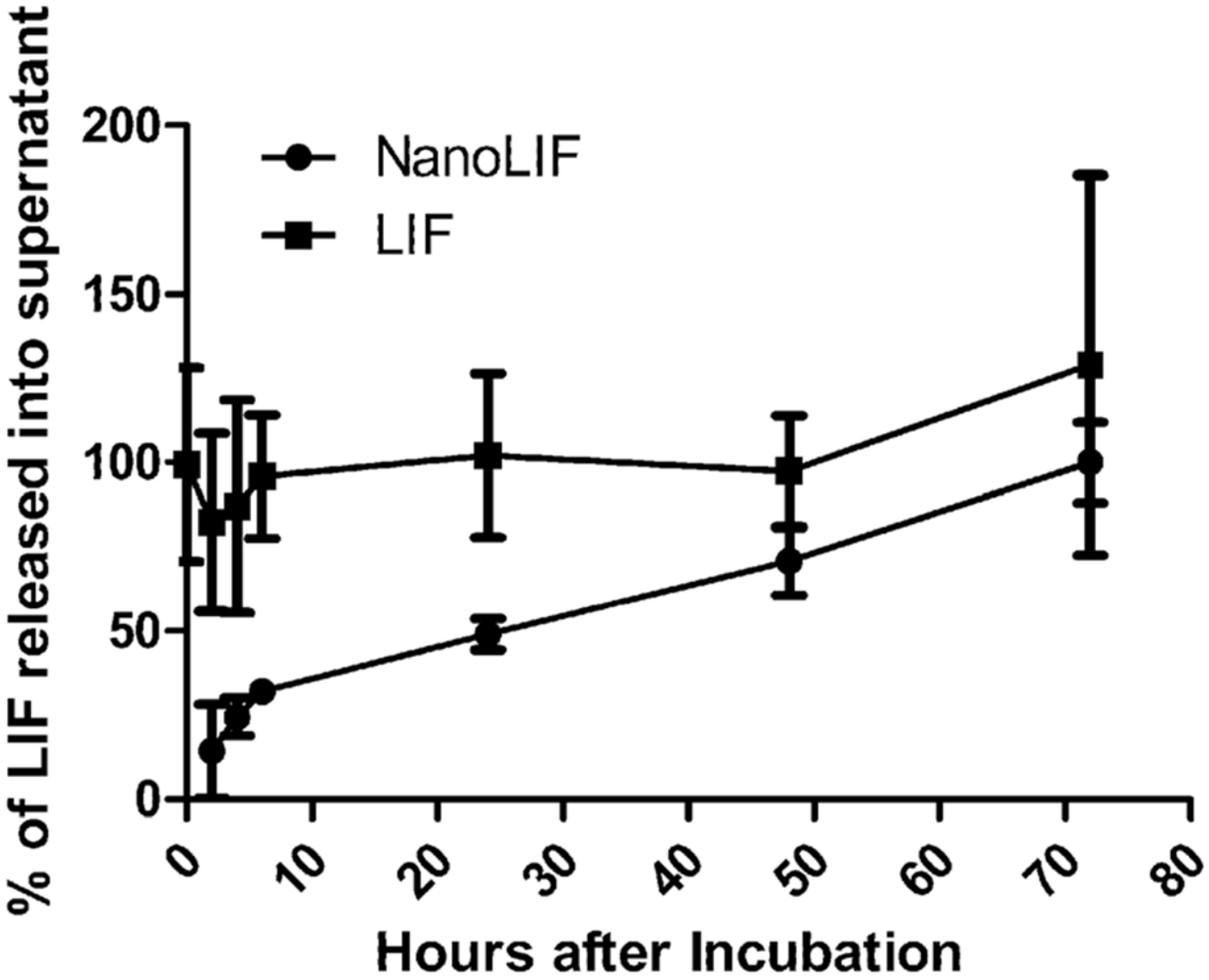

Fig. 6.

There was a significant change in the quantity of LIF released from NanoLIF particles over the 72 h period (*$p < 0.0001$). However, the concentration of LIF in the supernatant was not significantly altered over this period ($n = 3$ measurements per time point).

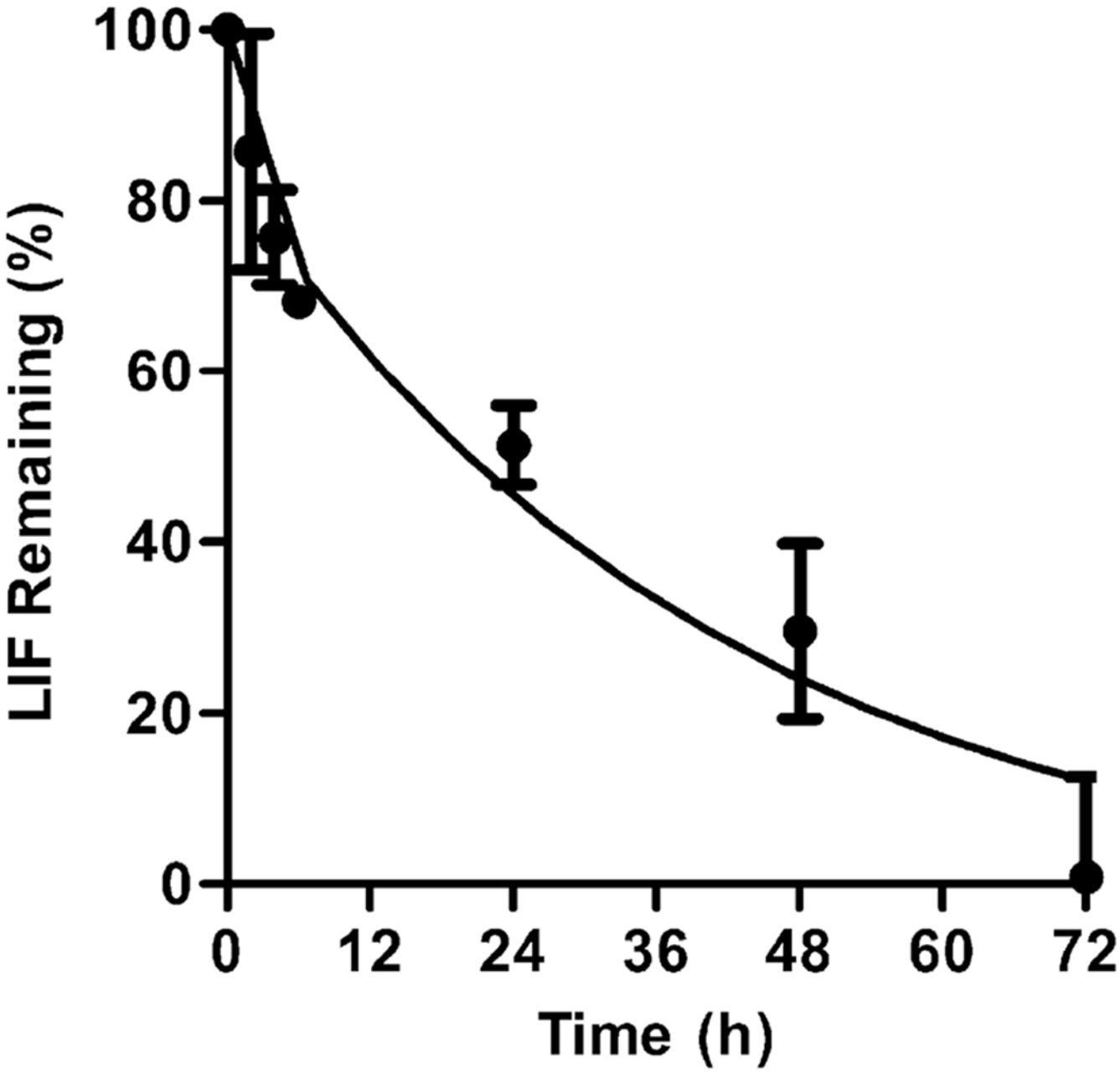

Fig. 7.

The pattern of LIF release from the NanoLIF particles over a 72 h time period was closely resembled a second order exponential decay pattern (n = 3 measurements per time point; $p < 0.05$).

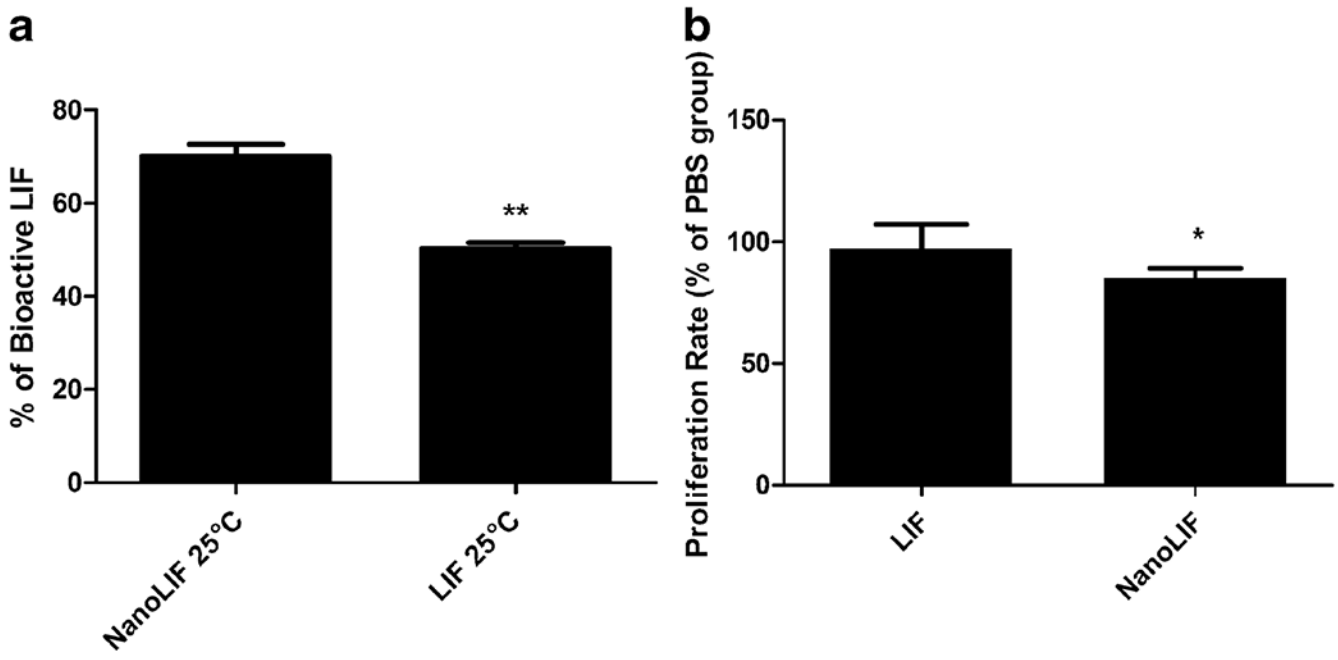

Fig. 8.

NanoLIF reduced degradation of biologically active LIF after incubation at 25°C for 12 h as measured by (**a**) ELISA (*$p < 0.001$; n = 3 measurements per group) and (**b**) the M1 cell proliferation assay (*p < 0.05; $n = 4$ independent experiments).

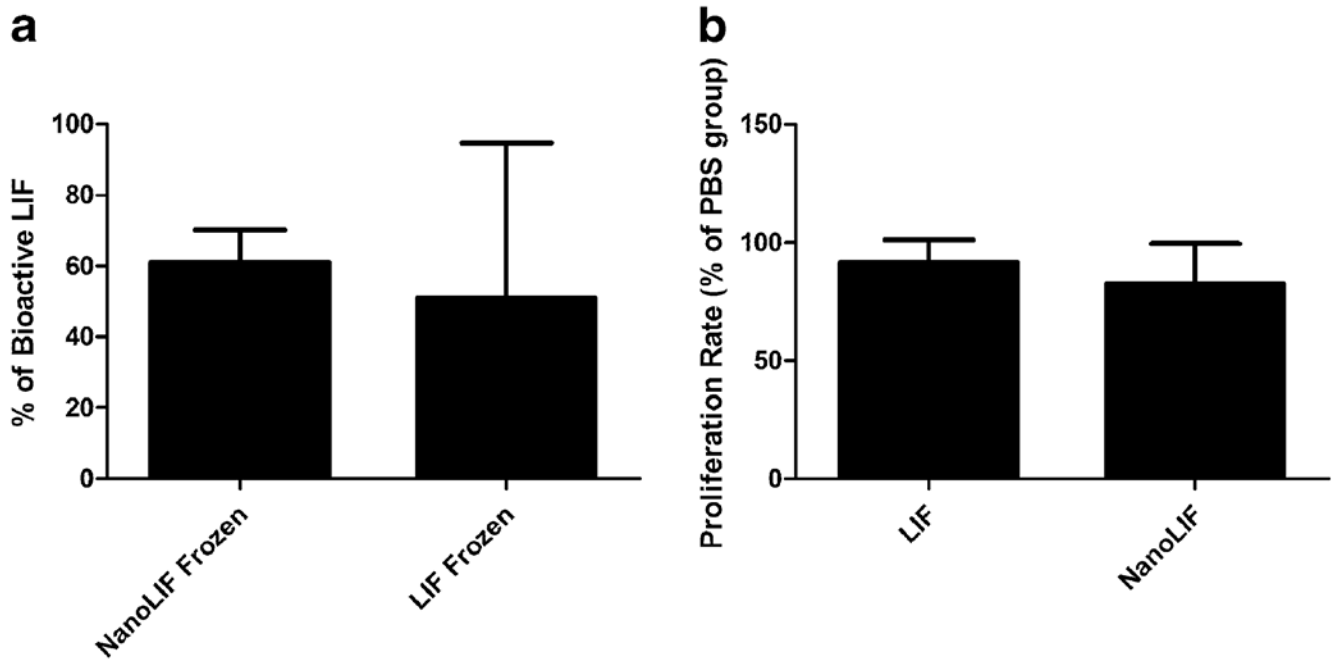

Fig. 9.

(**a**) NanoLIF did not significantly reduce the degradation of biologically active LIF after one freeze/thaw cycle as measured by the ELISA (n = 3 measurements per group). (**b**) Although there was a trend towards decreased M1 proliferation after treatment with NanoLIF this decrease was not statistically significant ($p > 0.05$; $n = 5$ independent experiments).

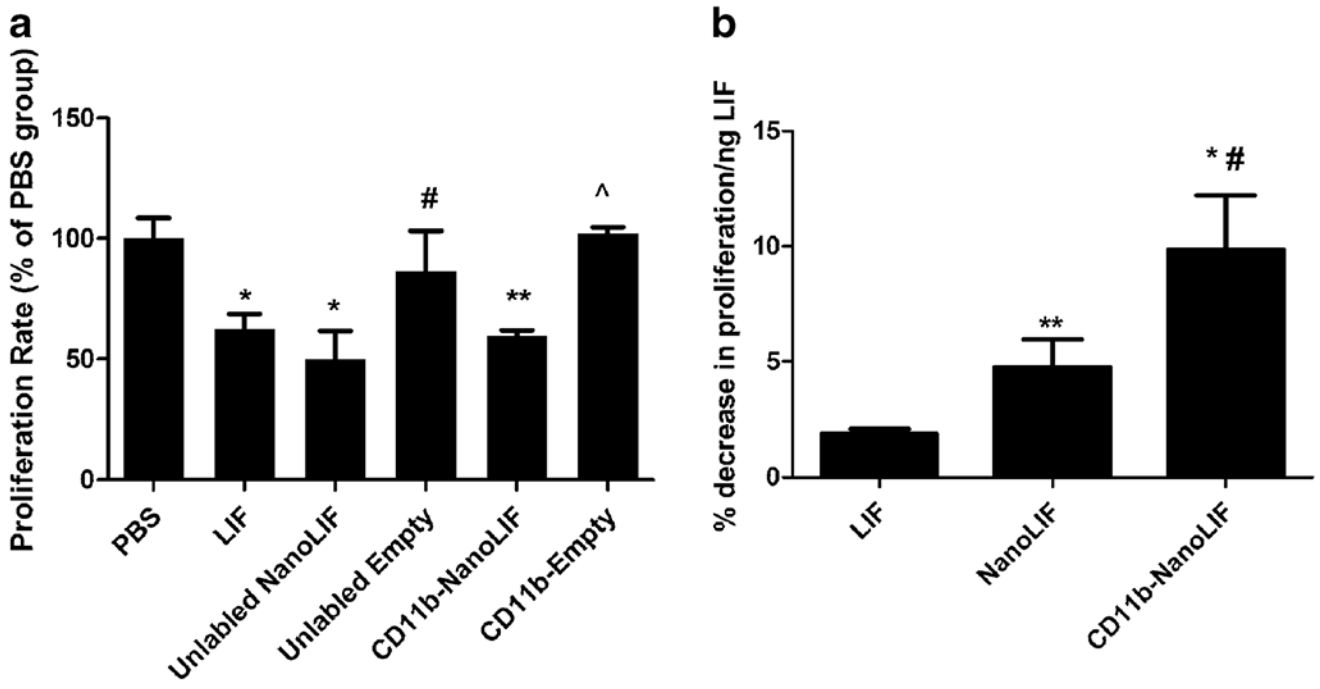

Fig. 10.

(**a**) LIF, NanoLIF (*p < 0.05), and CD11b-NanoLIF (**p < 0.01) significantly reduced the proliferation of M1 cells compared to PBS, while NanoLIF (#p < 0.05) and CD11b-NanoLIF (^p < 0.001) significantly reduced proliferation compared to their empty counterparts. (**b**) When reduction in M I proliferation was normalized to ng/LIF (*p < 0.05) NanoLIF and CD11b-NanoLIF were significantly more efficient than LIF (*p < 0.01) while CD11b-NanoLIF was significantly more efficient than NanoLIF (#p < 0.05; n = 3 independent experiments).

Table I

Physical Characteristics of NanoLIF and CD11b-NanoLIF

Formulation	Diameter (nm)	Zeta Potential (mV)	Polydispersity Index (PDI)	log(CMC)	CMC (μg/ml)
NanoLIF	52.3 ± 2.7	−2.6 ± 0.6	0.34 ± 0.04	−1.03 ± 0.09	93
CD11b-NanoLIF	39.9 ± 3.3*	−2.9 ± 0.2	0.32 ± 0.03	−1.51 ± 0.13	31*

Differences in size and CMC are statistically significant (*$p < 0.01$), while differences in zeta potential and PDI are not statistically significant ($p > 0.05$; $n = 3$ samples per group)

Table II

Loading and Encapsulation Efficiency of NanoLIF and CD11b-NanoLIF

Formulation	LIF Loading Efficiency (% * 10^3)	LIF Encapsulation Efficiency (%)
NanoLIF	6.0 ± 0.2	9.6 ± 0.2
CD11b-NanoLIF	15.0 ± 0.2*	24.1 ± 0.4*

All measurements are reported as mean ± standard deviation ($n = 3$). Differences in LIF loading efficiency and encapsulation efficiency were statistically significant (*$p < 0.0001$)

Table III

Release Kinetics of LIF from NanoLIF

	k_{fast} (hr^{-1})	k_{slow} (hr^{-1})	$t_{1/2,fast}$ (hr)	$t_{1/2,slow}$ (hr)	% Fast
First Order Exponential	0.034 ± 0.006	–	20.3 ± 4.4	–	–
Second Order Exponential	0.62 ± 0.88	0.024 ± 0.005	1.2 ± 1.3	28.9 ± 7.7	16.3 ± 8.9

The quantity of LIF released over the course of 72 h was used to calculate the release kinetics of NanoLIF